Project acronym:	**Geo-Drill**		
Project title:	Development of novel and Cost-Effective drilling technology for geothermal Systems		
Activity:	LCE-07-17-Renewables		
Call:	H2020-LC-SC3-2018-RES-TwoStages		
Funding Scheme:	RIA	**Grant Agreement No:**	815319
WP 2	**Development of Materials and Coatings**		

D2.8 - Report on HEA and cermet alloy based coating synthesis

Due date:	30/09/2020 (M18)	
Actual Submission Date:	03/02/2021	
Lead Beneficiary:	TWI	
Main authors/contributors:	TWI	
Dissemination Level[1]:	PU	
Nature:	REPORT	
Status of this version:		**Draft under Development**
		For Review by Coordinator
	X	**Submitted**
Version:	1.0	
Abstract	This deliverable reports on development of suitable deposition process parameters using high velocity oxygen fuel (HVOF) spraying for cermet and high entropy alloys (HEA) materials, focusing on their microstructure and hardness characteristics.	

REVISION HISTORY

Version	Date	Main Authors/Contributors	Description of changes

This project has received funding from the *European Union's Horizon 2020 research and innovation programme* under grant agreement No 815319

[1] Dissemination level security:

PU – Public (e.g. on website, for publication etc.) / **PP** – Restricted to other programme participants (incl. Commission services) / **RE** – Restricted to a group specified by the consortium (incl. Commission services) / **CO** – confidential, only for members of the consortium (incl. Commission services)

This project has received funding from the European Union's Horizon 2020 program Grant Agreement No 815319. This publication reflects the views only of the author(s), and the Commission cannot be held responsible for any use which may be made of the information contained therein.

Summary

In this deliverable, work is described to develop suitable deposition process parameters using high velocity oxygen fuel (HVOF) spraying for cermet and high entropy alloys (HEA) materials, focusing on their microstructure and hardness characteristics. Several combinations of spray parameters were studied for each powder to identify a suitable deposition process. Both hardness and microstructural characterisation were carried out for each coating type and each spray parameter combination; the best ones were selected to prepare test coupons for WP3 testing, including:

- Two cermet coatings including WC-Ni and WC-CrC-Ni, with hardness of 1077±60 $HV_{0.3}$ and 994±121 $HV_{0.3}$, respectively;
- One high entropy alloy (HEA) coating with a hardness of 558±61 $HV_{0.3}$.

Objectives Met

The work described in this report contributes to the following WP2 objective:

- To synthesise materials, coatings and develop coating technique for Geo-Drill components.

CONTENTS

1. INTRODUCTION

In this deliverable report, work is described to develop coating systems using high velocity oxygen fuel (HVOF), to be tested in simulated geothermal environments in WP3, including cermet and high entropy alloy (HEA) coatings. Development of the process parameters has been defined in the KPI report submitted earlier (D1.5: Geo-Drill KPIs).

In deliverable D2.4 "Report on drill bit tooth, fluidic oscillator, and stabilizer coating manufacture and properties", two cermet materials were studied, namely WC-Co-Cr and CrC-NiCr. Another two different cermet materials were selected in this report, WC-Ni and WC-CrC-Ni. Both use Ni as a metallic binder. Co has been the dominant addition to cermets (metal-ceramic composites) to achieve very good adhesion with WC in the solid state. However, the high price of Co, together with the need to improve the performance of cermets under severe working condition such as corrosion, has promoted Ni as an alternative binder [1]. Powder WC-CrC-Ni incorporates two kinds of carbides, WC and Cr_3C_2. It is considered to bridge the gap between WC-Co(Cr) and Cr_3C_2-NiCr coatings due to the excellent oxidation and corrosion resistance of Cr_3C_2 [2].

High entropy alloys (HEAs) are a new class of materials, which comprise at least five elements that bring together their unique properties to create a new and better material. The high mixing entropy allows them to have a lower free-energy and higher phase stability. Therefore, HEAs have the tendency to form simple solid phase, such as FCC and BCC phases rather than intermetallic compounds, and their microstructures retain good thermal stability [3]. A range of researchers have revealed their findings regarding the remarkable properties of high entropy alloys, such as high strength and hardness, excellent corrosion and wear resistance, and wide-temperature range applications [4,5]. However, the potential use of HEA in geothermal environments has not yet been significantly explored.

The process described in D2.4 Section 2.2, HVOF using the JP5000 system, was also used for this Task. The high velocity and lower flame temperature are especially favourable for spraying cermet and HEA materials. Coating performance were evaluated by analysing coating porosity (the lower the better), microstructure (i.e. appearance of cracks, pores or other defects) and hardness to select the preferred process parameters for preparing test coupons to be further tested in WP3.

2. APPROACH

2.1 Materials

2.1.1 Powder

To maintain the same principle as D2.4 for achieving higher technology readiness levels (TRLs) of the drilling system developed in the project and to maintain a consistent coating quality in the geothermal environment, powders were selected in this Task aiming to satisfy the following criteria:

- Commercially available;
- To offer improved abrasion resistance and/or lower coefficient of friction at elevated temperature (minimum 250°C);
- To offer corrosion and erosion resistance at elevated temperature (minimum 250°C);
- To enable achieving a relatively smooth surface finish.

Among three powders selected for this Task, two cermet powders WC-Ni and WC-CrC-Ni are commercially available. However, HEA material is a recently developed material and is not commercially available yet. Furthermore, synthesising a new type of HEA powder from various metal combinations takes an extensive amount of work. The timeline and budget in Geo-Drill would not allow such extra work; the consortium therefore decided to use a result that was already established in another H2020 project, Geocoat (GA No: LCE-

GA-2018-764086). The composition of HEA powder, CoCrFeNiMo0.85, whose corresponding coating performed the best in Geocoat, was selected and was then mechanically alloyed by MBN Nanomaterialia S.p.A. Information about the powders in this report is listed in Table 1 and

Table 2.

Table 1 Selected cermet powders with properties suggested by suppliers.

TWI ID	Powder	Chemistry	Size, µm	Supplier	Erosion	Abrasion	Wear	Corrosion	Servicing temperature, °C
4286	SX477	90%WC10%Ni	-44 / +10	GTP	Y	Y	Y	-	500
4287	SX199	WC-Cr3C2-Ni	-54 / +10	GTP	Y	Y	Y	-	500

Table 2 Composition of high entropy powder (CoCrFeNiMo0.85, TWI ID: 4293)

Composition	Co	Cr	Fe	Mo	Ni
Mol ratio	1	1	1	0.85	1
at%	20.62	20.62	20.62	17.53	20.62
Wt%	19.19	16.94	18.19	26.56	19.12

2.1.2 Substrates

As in D2.4, bright mild steel substrates (40×40×6 mm) were used for DoE trials in this report. Once the best parameters were determined, coatings were then deposited onto substrates (817M40T, 440B, and 835M30) to be tested in WP3. Steel specification and nominal compositions are listed in Table 3.

Table 3 Material specifications and nominal compositions of steel substrates

Steel types	Compositions
Bright mild steel (EN3B)	C 0.180, Si 0.160, Mn 0.770, P 0.009, S 0.007, Cr 0.060, Mo 0.040, Ni 0.080, Cu 0.012, Al 0.009, Fe bal.
34CrNiMo6 (EN24T)	C 0.430, Si 0.310, Mn 0.590, P 0.009, S 0.033, Cr 1.200, Mo 0.220, Ni 1.400, Pb 0.0007, Cu 0.200, Sn 0.014, Ca 0.0029, N 0.012, Nb 0.005, Ti 0.0048, V 0.010
440B	C 0.83, Si 0.43, Mn 0.40, P 0.029, S 0.001, Cr 0.001, Cr 16.7, Mo 0.59
835M30 (EN30B)	C 0.310, Si 0.260, Mn 0.550, P 0.008, S 0.0047, Cr 1.190, Mo 0.330, Ni 4.100, Cu 0.150, Sn 0.008,Al 0.024, Ti 0.0014, N 0.006, Ca 0.005, V 0.003

2.2 HVOF spray process

The Tafa JP5000 HVOF system was used for coating deposition in this report and spray procedures were as described in D2.4. Powder was fed radially into the gun and liquid kerosene was used as fuel. As powders in this

task either present a high level of fine particles or have irregular shape, a three-way powder splitter was used to avoid pick-up in the nozzle. Fixed spray parameters used for each powder are given in Table 4.

The development of coatings described in this report reflects work described in the RP1 report and the RP1 review. From D2.4 report, Section 1.2, thermal spray is a very complex process. It was deemed not appropriate to attempt to use techniques such as adaptive design of experiments (DoE) and metamodeling to explore various parameter combinations for so many material varieties, which was partly due to high cost and long timescale. A simplified but more effective approach was used to develop suitable parameters for each material type. As a good knowledge was obtained in Task 2.3(D2.4 report) on coating microstructure under different parameters for various material types, including nozzle length, powder feeder, spray distances and spray angles. The DoE spray parameters for this task only focus on fuel/oxygen flow rates, which is considered to be critical for getting a suitable combustion environment to produce a good quality coating (Table 5-Table 7).

Bright mild steel substrate (40×40×6 mm) was used for all the DoE optimisation. Before spraying, all the substrates were ground flat and then were grit-blasted to remove surface contaminants and to create a rough surface for better adhesion. Surface preparation parameters were:

- Blast media: alumina;
- Mesh size:60;
- Running air pressure:60 psi;
- Stand-off distance: 80mm;
- Abrasive nozzle: Ø=8mm ID.

The roughened surface was then cleaned using compressed air and alcohol. Coating deposition was carried out immediately after grit-blasting and cleaning.

Table 4 Fixed spray parameters for JP5000

Spray parameter	WC-Ni (SX477)	WC-CrC-Ni (SX199)	HEA (CoCrFeNiMo0.85)
Powder carrier Gas	Argon	Argon	Argon
Powder feed rate, rpm	350	250	150
Carrier gas flow rate, scfh	28	28	28
Gun transverse speed, mm/s	900	900	900
Increment, mm	5	5	5
No of passes	45	30	36
Nozzle, inch	6	6	4
Specimen cooling	air	air	air

Table 5 DoE conducted for HVOF with WC-Ni powder

Run #	Oxygen flow, SLPM	Kerosene flow, SLPM	Spray distance, mm	Angle, °	Spray sheet
281WC1	920	0.400	350	90	20-123
281WC2	873	0.375			20-125
281WC3	920	0.375			20-126
281WC4	920	0.350			20-127

Table 6 DoE conducted for HVOF with WC-CrC-Ni powder

Run #	Oxygen flow, SLPM	Kerosene flow, SLPM	Spray distance, mm	Angle, °	Spray sheet
282WCr1	920	0.400	350	90	20-128
282WCr2	873	0.375			20-129
282WCr3	920	0.375			20-130
282WCr4	920	0.350			20-131

Table 7 DoE conducted for HVOF with HEA powder

Run #	Oxygen flow, SLPM	Kerosene flow, SLPM	Spray distance, mm	Angle, °	Spray sheet
283HEA1	920	0.355	355	90	20-187
283HEA2	873	0.330			20-188
283HEA3	873	0.355			20-189
283HEA4	873	0.375			20-190

2.3 Characterisation

2.3.1 Overview

The characteristics of deposited samples was assessed in terms of coating characteristics and mechanical performance using a combination of methods, including SEM/EDX, optical microscopy, micro-hardness, adhesion test etc, in order to select the best coatings.

2.3.2 Surface roughness

Samples were measured using an Alicona InfiniteFocus SL 3D surface profilometer. The surface information was gathered by moving the optics relative to the sample while continuously imaging the surface. Height information was then determined from the regions of the images which were in focus. The measurement was done based on BS EN ISO 4288. At least three measurements were done for each sample and an average was taken.

2.3.3 Deposition efficiency

Deposition efficiency (D.E.) was measured mainly by weight deposited per minute. It was calculated from weight changes of samples before and after being sprayed. At least three specimens were measured for each sample and an average was taken.

2.3.4 Coating porosity

Coating porosity was measured according to ASTM E2109-01:2007 Standard. The cross-sectioned samples were cold-mounted in epoxy, ground with silicon carbide paper with progressively finer grit size, then polished with diamond (3 and 1 µm) and colloidal silica (0.02 µm) suspensions. Optical microscopy was used to take microstructure images on their polished cross-section surfaces. Porosity was calculated by area fraction analysis and thresholding of at least twenty micrographs using ImageJ software. An average value was taken.

2.3.5 Microstructure characterisation

For powder and coating microstructural analysis, scanning electron microscopy (SEM) equipped with energy dispersive X-ray spectroscopy (EDX) was used. Images at different magnifications were taken mainly at backscattered mode for higher contrast between pores, oxide areas and metal matrix. EDX spectroscopy was used while imaging on SEM to obtain the elemental compositions at different areas of the sample cross-sections.

2.3.6 Hardness

Micro-hardness measurement was taken on the prepared coating cross-sections using a Duramin Vickers hardness tester, manufactured by Struers in accordance with BS EN ISO 6507 part 1. A load of 300g was used and at least ten indents were made along the coating length. The hardness value was expressed as an average value with a standard deviation.

2.3.7 Adhesion strength

Adhesion strength of deposited coatings was measured using pull-off adhesion testing according to ASTM C633-1. The test determines adhesion strength of a coating to a substrate, or the cohesive strength of the coating, in tension normal to the surface. The coated samples were bonded onto dollies with testing area of 25.4mm diameter. The load was applied using an Instron machine, up to the point at which bonding failure occurred. The joint was then examined to determine the location of failure and classified as occurring at either the coating to the substrate interface, within the coating or within the epoxy adhesive. Five samples were tested for each coating and the failure stress was expressed as a mean of five results with a standard deviation.

3. RESULTS AND DISCUSSION

3.1 Cermet

3.1.1 WC-Ni

3.1.1.1 Powder

The microstructure of powder SX477 WC-Ni and its EDX analysis are shown in Figure 1 It can be seen that the agglomerated powder presents mostly spherical particles with a small level of irregular-shaped ones. Moreover, it also contains a range of finer particles with size less than 15µm, indicating that the spray process for this powder should be very carefully selected to avoid nozzle blocking. Therefore, a three-way powder splitter was used in order to get better powder distribution. Analysis of the cross-section surface shows that the powder has homogeneously distributed two phases: bright areas of WC particles with dark regions of Ni binder.

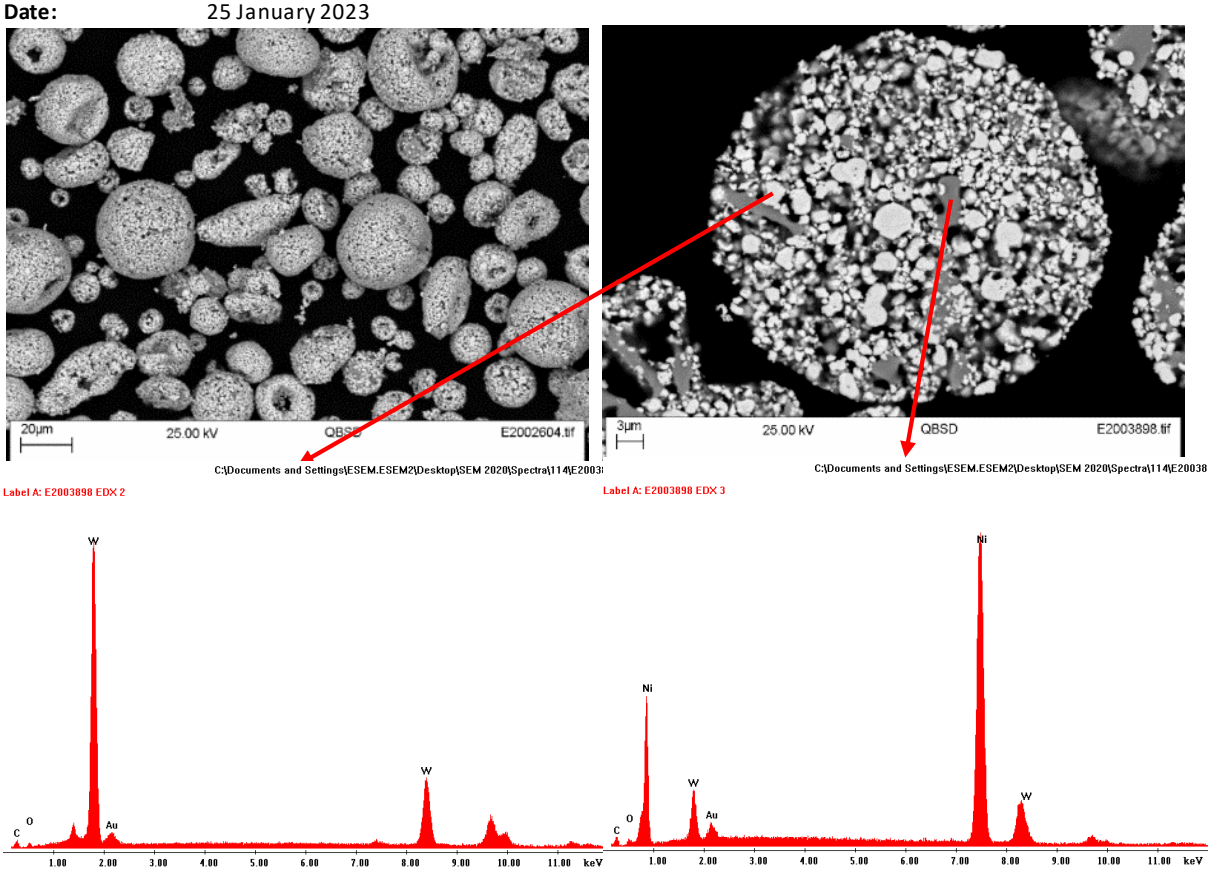

Figure 1 SEM and EDX analysis of powder 4286, SX477 WC-Ni (top-left: as-received surface, top-right: cross-sectioned surface)

3.1.1.2 Coatings

When being deposited under various oxygen and fuel flow rates, all four WC-Ni coatings present a very uniform structure (Figure 2-Figure 5). Though a few delaminated pieces are found on the top surface of these coatings, no visible cracks can be seen. This might be formed during metallographic preparation due to the brittleness of WC particles. Different oxygen and fuel flow rates do not seem to influence surface roughness much, with the Ra of all the coatings in the range of about 3.6 to 3.9µm (Table 8). However, the porosity varies from 2.0 to 3.4%, deposit efficiency varies from 33 to 39% and micro-hardness varies from 1059 to 1113$HV_{0.3}$ (Table 9). Higher oxygen flower rate seems to be favourable for this powder to get a denser coating. Of the four coatings, 281WC3 was selected as the best due to its lowest density and good hardness

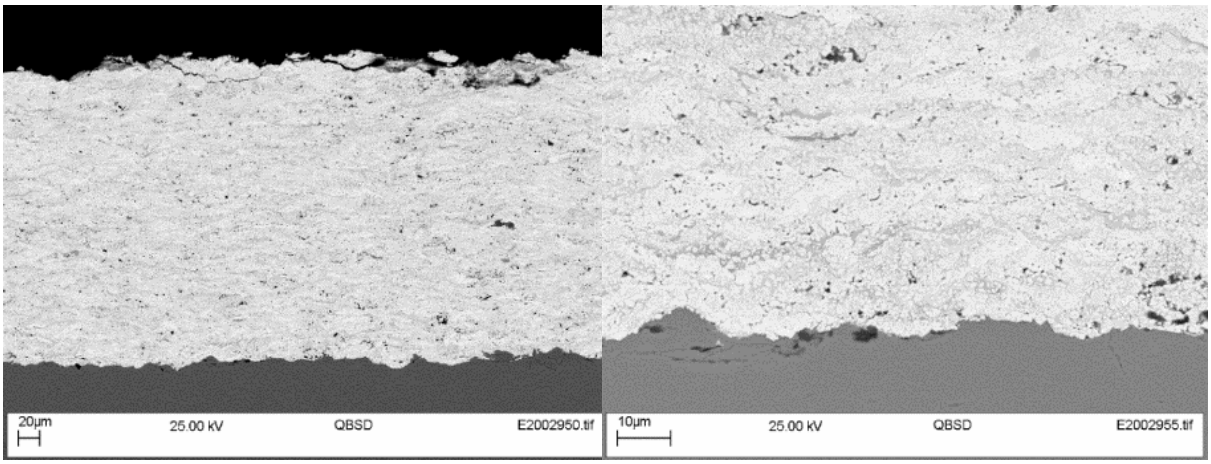

Figure 2 SEM micrographs of Coating 281WC1 under back-scatter mode

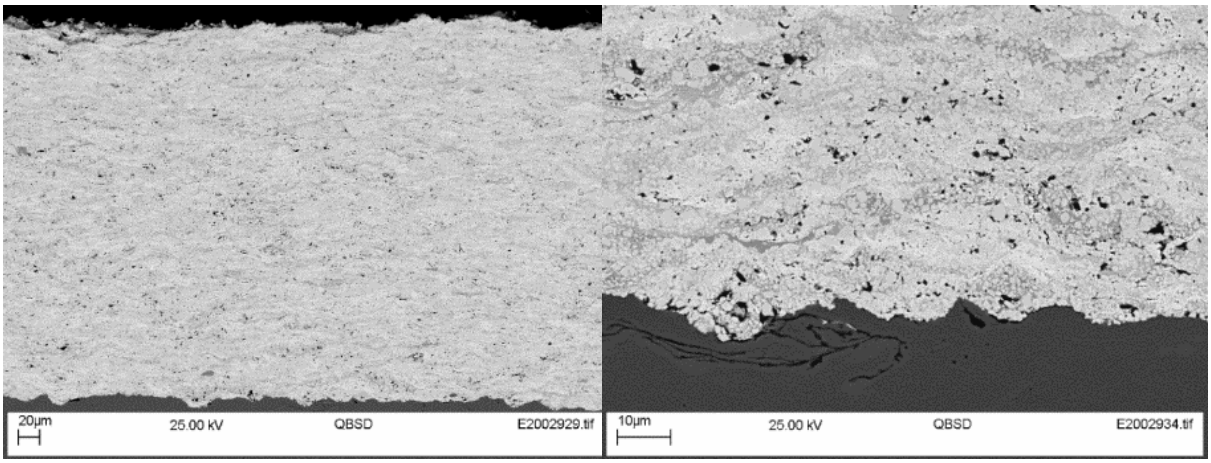

Figure 3 SEM micrographs of Coating 281WC2 under back-scatter mode

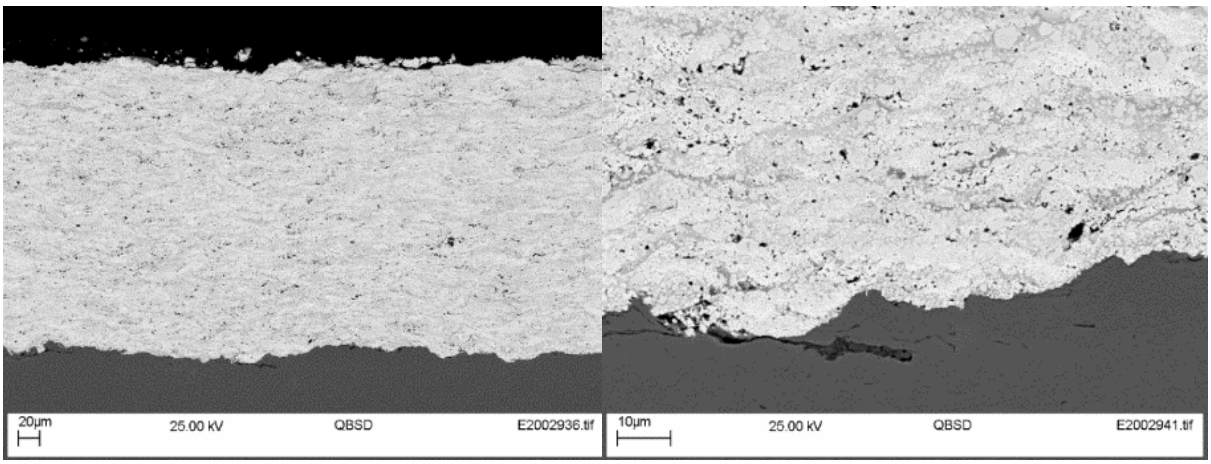

Figure 4 SEM micrographs of Coating 281WC3 under back-scatter mode

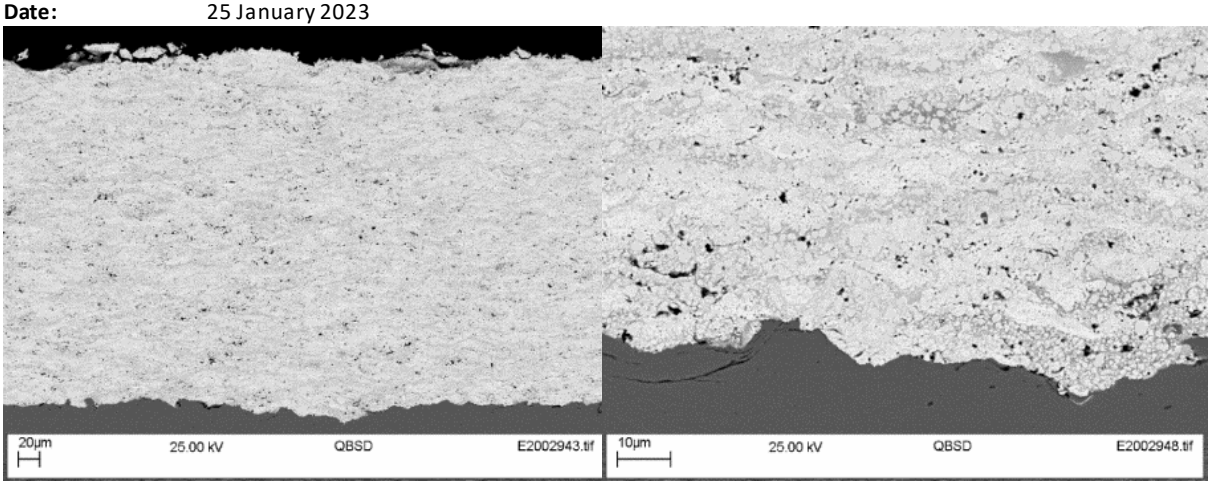

Figure 5 SEM micrographs of Coating 281WC4 under back-scatter mode

Table 8 Coating surface roughness of DoE matrix with 4286 - SX477 WC-Ni powder

Run #	Oxygen flow, SLPM	Kerosene flow, SLPM	Ra, µm		Rz, µm	
			Ave	Dev	Ave	Dev
281WC1	920	0.400	3.6	0.3	30.0	26.0
281WC2	873	0.375	3.6	0.4	28.6	26.2
281WC3	920	0.375	3.9	0.2	32.6	28.9
281WC4	920	0.350	3.9	0.3	26.8	29.7

Table 9 Test results of DoE matrix with 4286 - SX477 WC-Ni powders

Run #	Oxygen flow, SLPM	Kerosene flow, SLPM	Porosity, %		D.E., %	Hardness, $HV_{0.3}$	
			Ave	Dev		Ave	Dev
281WC1	920	0.400	3.2	0.5	34	1083	78
281WC2	873	0.375	3.4	0.5	39	1059	165
281WC3	920	0.375	2.0	0.4	33	1077	60
281WC4	920	0.350	2.9	0.4	39	1113	80

3.1.2 WC-CrC-Ni

3.1.2.1 Powder

The microstructure of powder SX199 WC-CrC-Ni and its EDX analysis on the as-received and cross-sectional surfaces are shown in Figure 6 and Figure 7, respectively. The powder comprises a range of fine spherical particles with size less than 15µm, therefore a three-way powder splitter was also used for this powder to eliminate nozzle blocking. From its cross-section analysis, this powder is blended with a mixture of WC and CrC particles, with different morphologies. Both WC and CrC particles use Ni as binder, as indicated in EDX analysis (Figure 7).

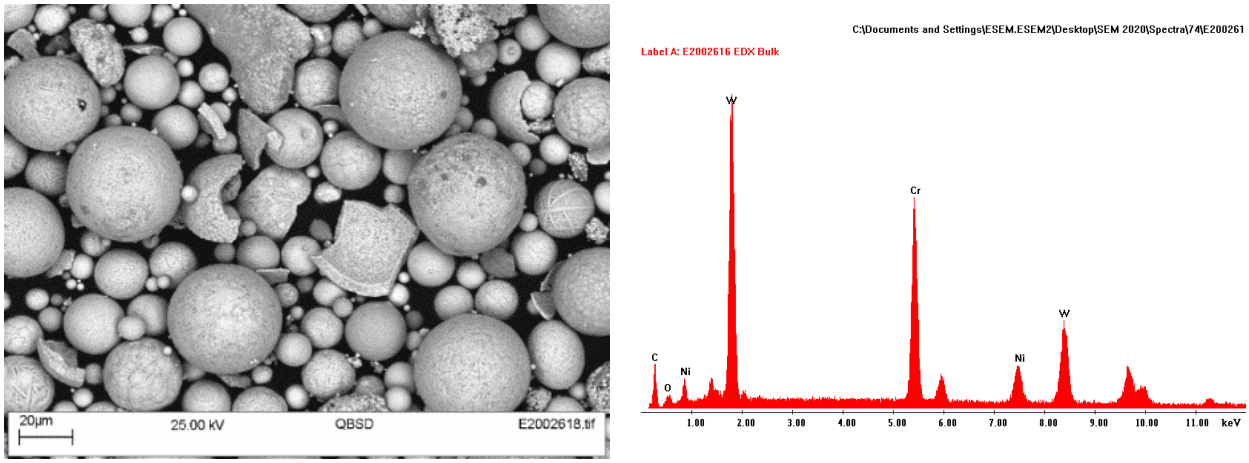

Figure 6 SEM and EDX analysis of as-received powder 4287, SX199 WC-CrC-Ni

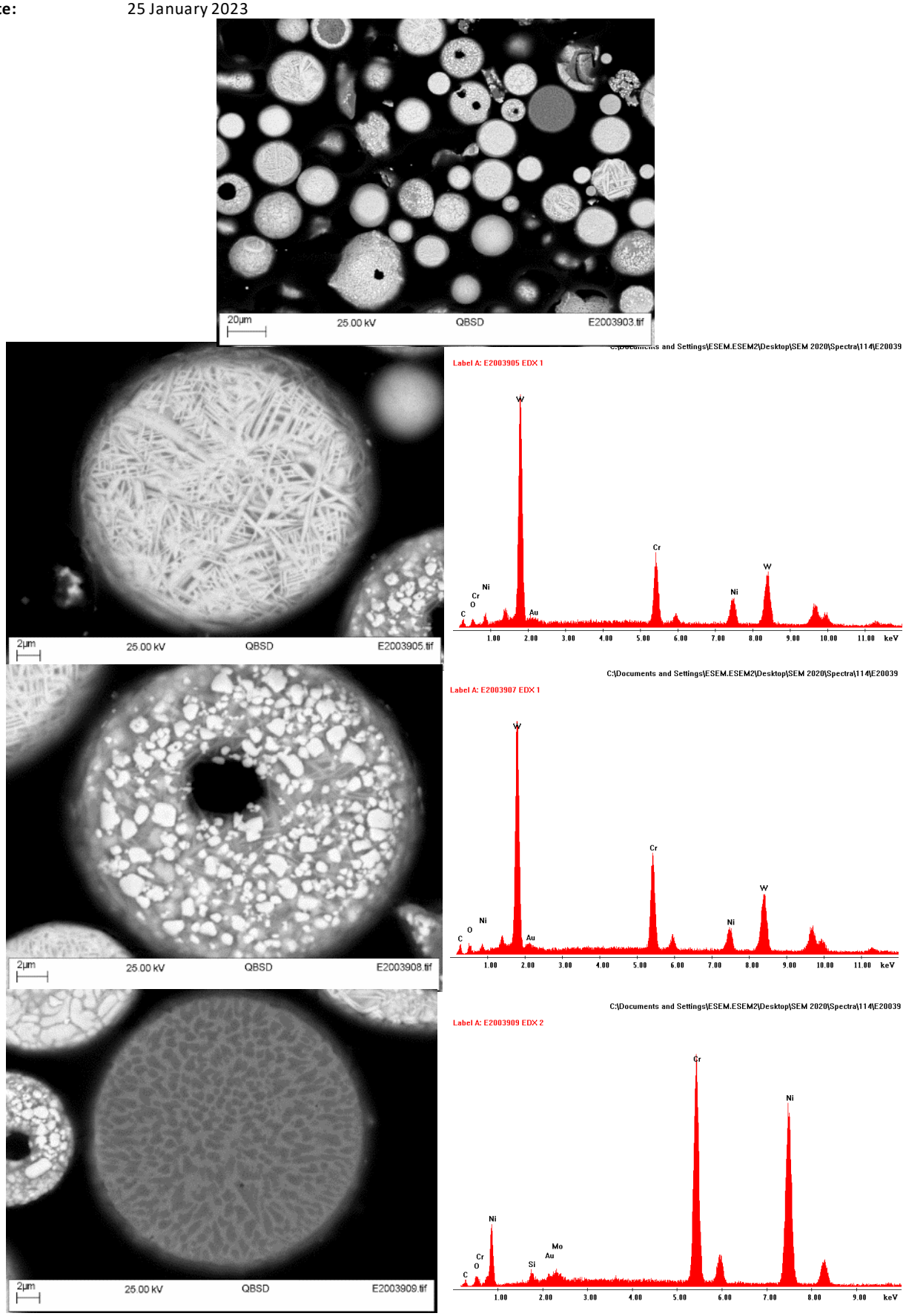

Figure 7 SEM and EDX analysis of cross-sectioned powder 4287, SX199 WC-CrC-Ni

3.1.2.2 Coatings

SEM analysis on WC-CrC-Ni coatings deposited from powder SX199 indicates a denser microstructure than those from WC-Ni powder SX477 (Figure 8-Figure 11). A few horizontal cracks are observed for coating 282WCr1 and 282WCr3. This was not seen for both WC coatings and CrC coatings developed in D2.4 and coating 281WC, it is assumed that this may be caused by different thermal conductivity of different materials. Therefore, careful selection of fuel and oxygen flow rates is critical for such blended powder.

When being deposited under different oxygen and fuel flow rates, WC-Cr-Ni coating has surface roughness Ra varies from 5.6 to 6.3 µm, porosity varies from 1.8 to 2.7%, deposit efficiency varies from 33 to 36%, and micro-hardness varies from 949 to 1074$HV_{0.3}$ (Table 10, Table 11). This blended powder has very similar deposit efficiency to WC-Ni powder. Though overall hardness for WC-Cr-Ni coating is slightly lower than WC-Ni coating due to addition of CrC particles, it offers a denser structure. This is deemed to be important for achieving good corrosion resistance of a coating. Of the four conditions, coating 282WCr4 was selected as the best due to its lowest porosity, high deposit efficiency, and good hardness.

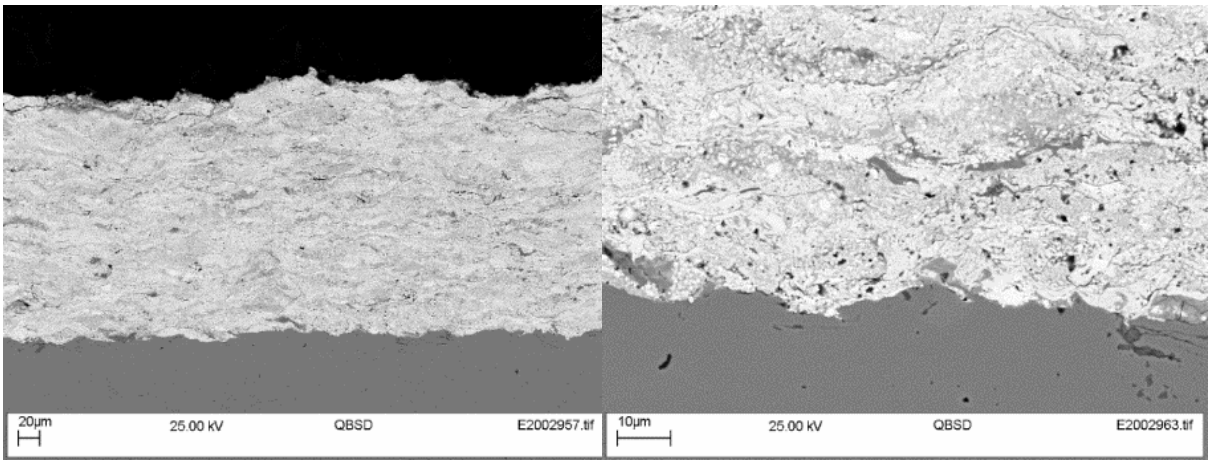

Figure 8 SEM micrographs of Coating 282WCr1 in back-scattered mode

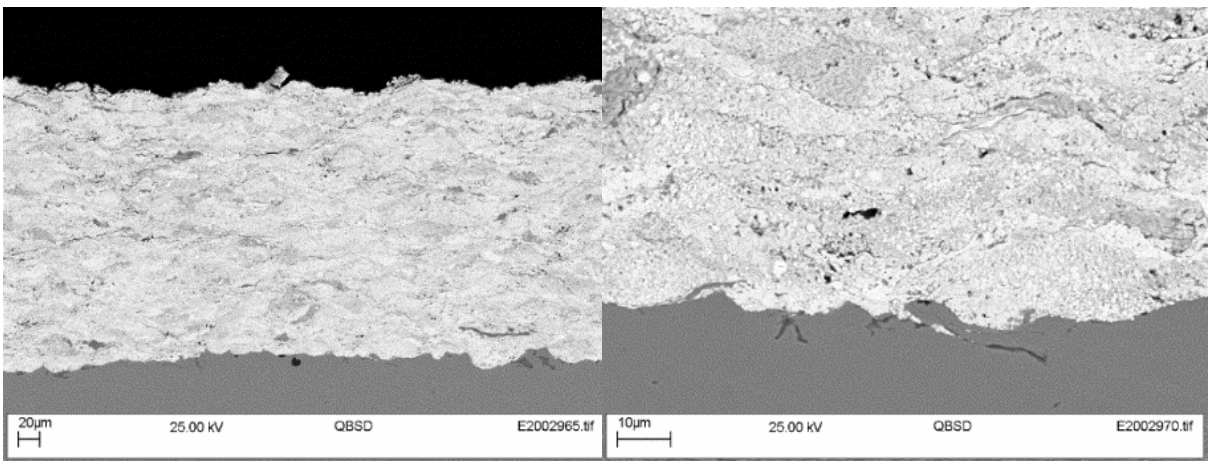

Figure 9 SEM micrographs of Coating 282WCr2 in back-scattered mode

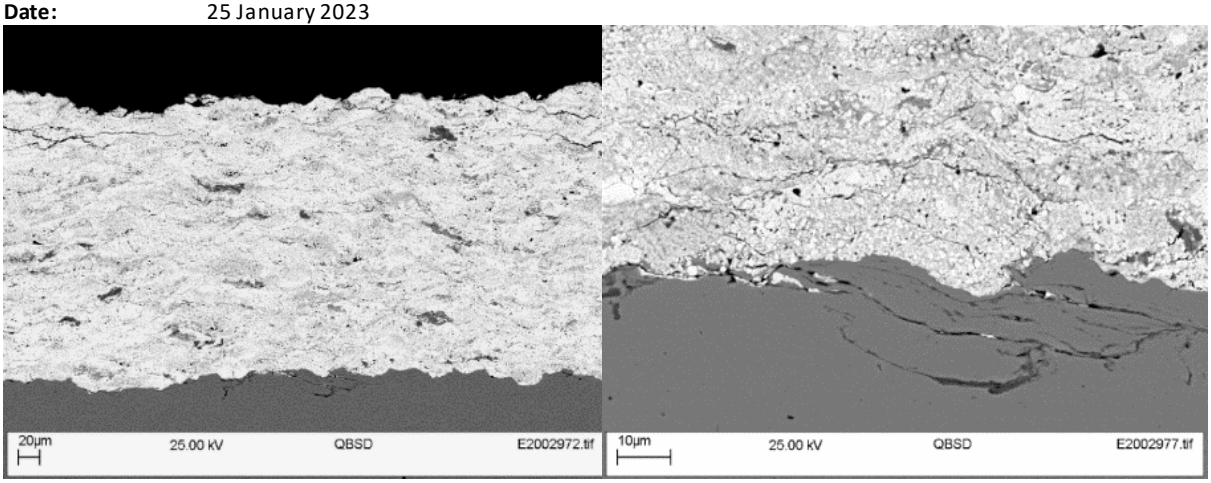

Figure 10 SEM micrographs of Coating 282WCr3 in back-scattered mode

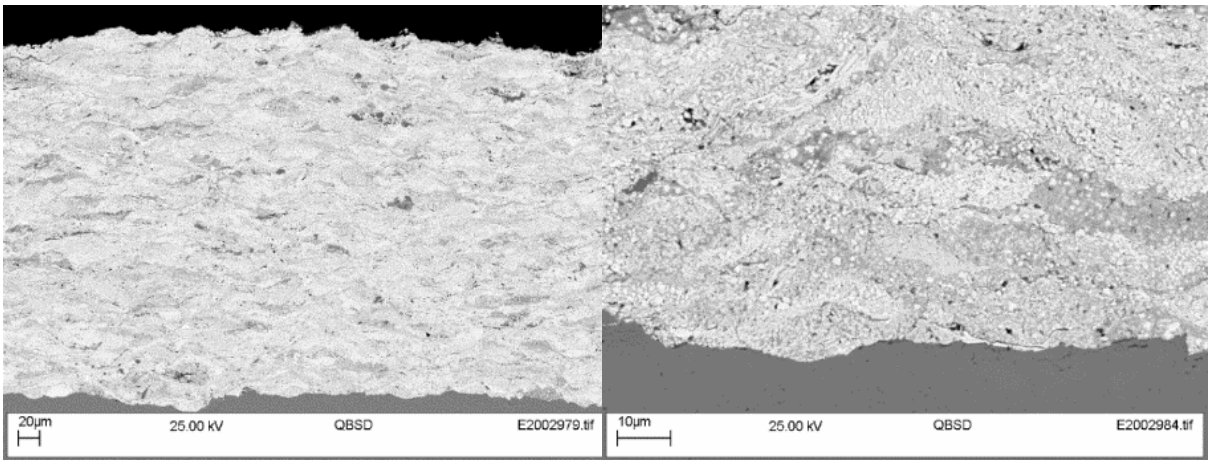

Figure 11 SEM micrographs of Coating 282WCr4 in back-scattered mode

Table 10 Coating surface roughness of DoE matrix with 4287 – SX199 WC-CrC-Ni powder

Run #	Oxygen flow, SLPM	Kerosene flow, SLPM	Ra, µm		Rz, µm	
			Ave	Dev	Ave	Dev
282WCr1	920	0.400	5.6	0.2	39.3	1.7
282WCr2	873	0.375	6.1	0.1	43.3	1.7
282WCr3	920	0.375	6.3	0.2	42.3	1.6
282WCr4	920	0.350	6.1	0.2	44.4	3.0

Table 11 Test results of DoE matrix with 4287 – SX199 WC-CrC-Ni powder

Run #	Oxygen flow, SLPM	Kerosene flow, SLPM	Porosity, %		D.E., %	Hardness, $HV_{0.3}$	
			Ave	Dev	%	Ave	Dev
282WCr1	920	0.400	1.9	0.4	33	980	110
282WCr2	873	0.375	2.7	0.6	35	949	152
282WCr3	920	0.375	2.0	0.3	33	1074	82
282WCr4	920	0.350	1.8	0.2	36	994	121

3.2 High entropy alloy (HEA)

3.2.1 Powder

The microstructure of HEA powder CoCrFeNiMo0.85 and its EDX analysis on as-received and cross-sectional surfaces are shown in Figure 12 and Figure 13, respectively. The powder presents a typical irregular shape of mechanically alloyed powder. From the thermal spraying perspective, feedstock with such a shape is known not to flow well. A three-way powder splitter and a shorter nozzle (4 inch) were used to eliminate the chance of nozzle blocking during the deposition process. The SEM image taken under back-scattered mode of the as-received condition shows that the powder is well-alloyed with uniform distribution of each element distributed on the surface (Figure 12). Further SEM and EDX analysis of the cross-sectioned surface indicates some small areas of inhomogeneity, with darker Cr-rich zones and brighter Mo-rich zones (Figure 13).

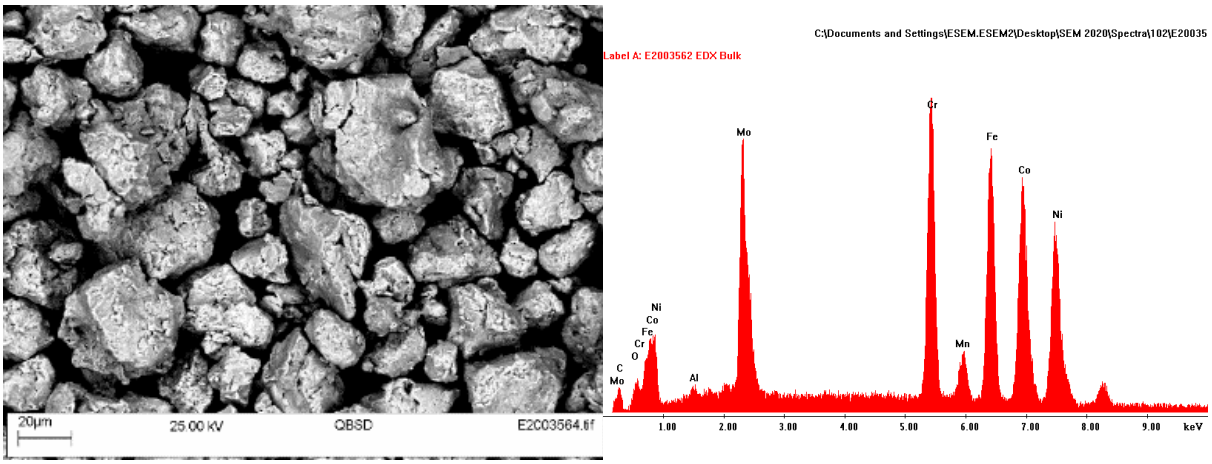

Figure 12 SEM and EDX analysis of as-received HEA powder 4293, CoCrFeNiMo0.85

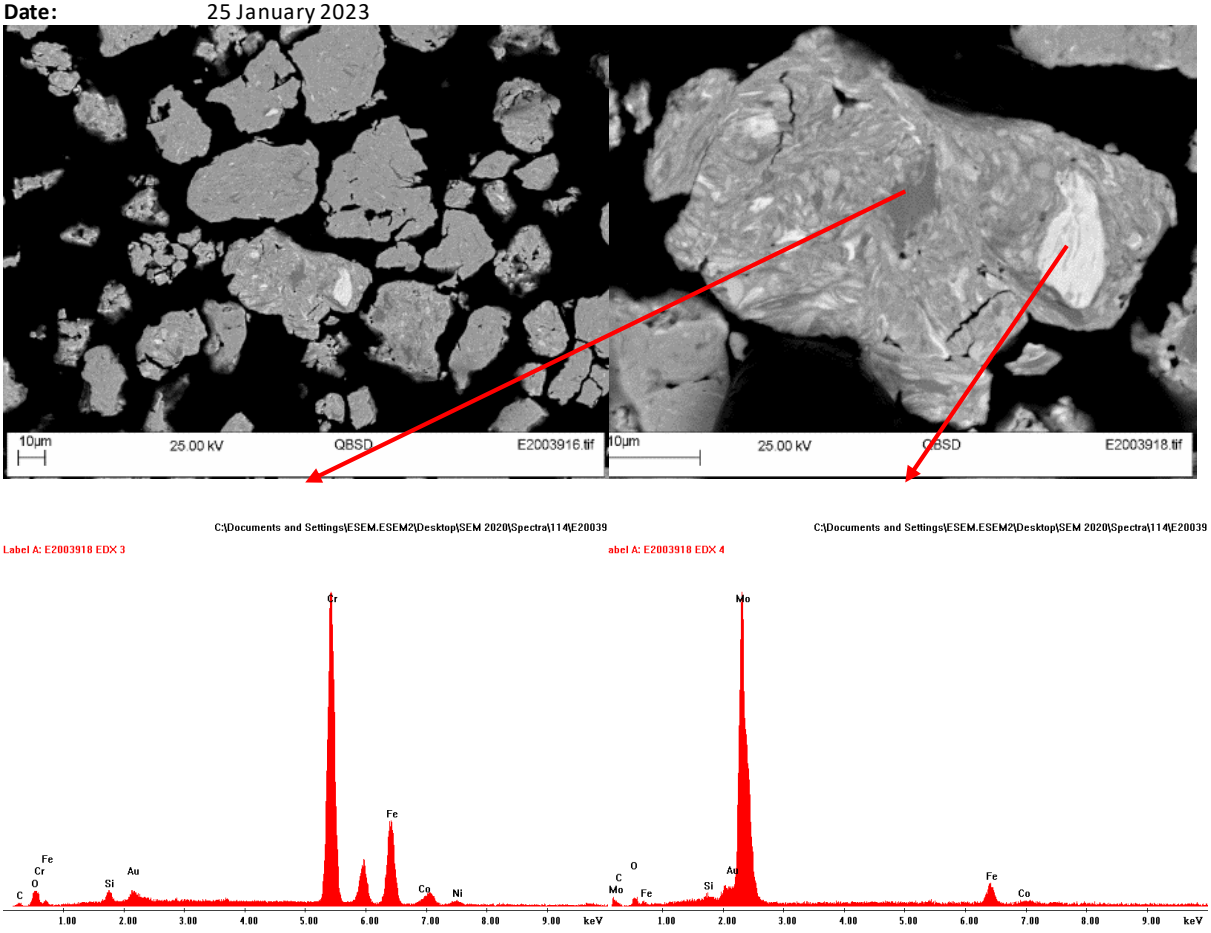

Figure 13 SEM and EDX analysis of cross-sectioned HEA powder 4293, CoCrFeNiMo0.85

3.2.2 Coatings

When being deposited under different oxygen and fuel flow rates, SEM analysis on cross-sectioned HEA coating surfaces shows that their microstructure is generally uniform with different features evenly distributed throughout the coating thickness (Figure 14-Figure 18). Further SEM and EDX analysis on sample 283HEA1 indicated that the HEA coating mainly comprises three phases: a) small area of Mo rich zone; b) small area of Cr rich zone; and c) main phase of well alloyed zone. The different phases seem to be randomly distributed in the coating when deposited under different spray conditions. No visible cracks are observed for all four coatings.

Surface roughness of all four HEA coatings is very similar and does not seem to be strongly affected by different fuel and oxygen flow rates (Table 12). Their adhesion strength varies between 43.7 and 59.2 MPa, which is much higher than other types of alloy coatings such as self-fluxing and amorphous coatings developed in D2.4 (Table 13). When sprayed under different oxygen and fuel flow rates, the porosity of the HEA coatings varies between 1.2 and 1.8%, deposit efficiency varies between 52 and 61% and micro-hardness varies from 528 to 575$HV_{0.3}$. When kerosene flow rate is increased at fixed oxygen flow rate, it offers lower chamber pressure and higher flame temperature, leading to higher density, but lower hardness in the coatings (Table 14, 283HEA2 vs 283HEA3 vs 283HEA4). Coating 283HEA3 was selected as the best due to its better overall coating characteristics, such as lower porosity, highest adhesion strength and deposition efficiency, high hardness and no visible presence of cracks.

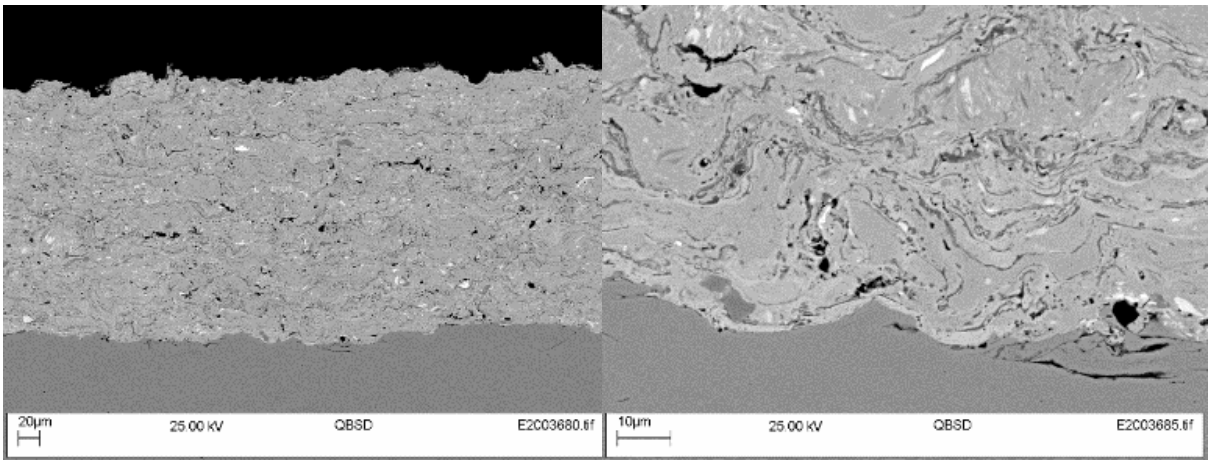

Figure 14 SEM micrographs of Coating 283HEA1 in back-scattered mode

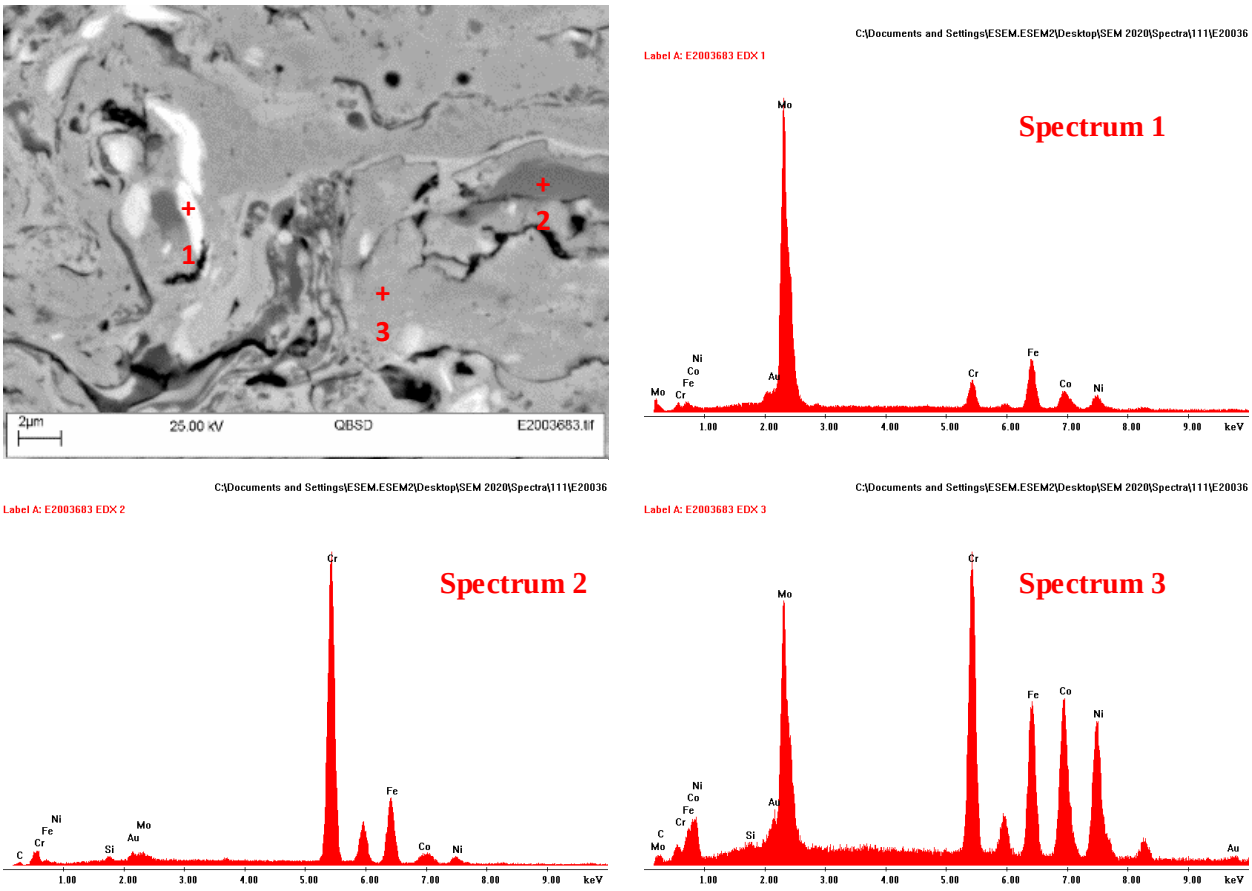

Figure 15 EDX analysis of coating 283HEA1

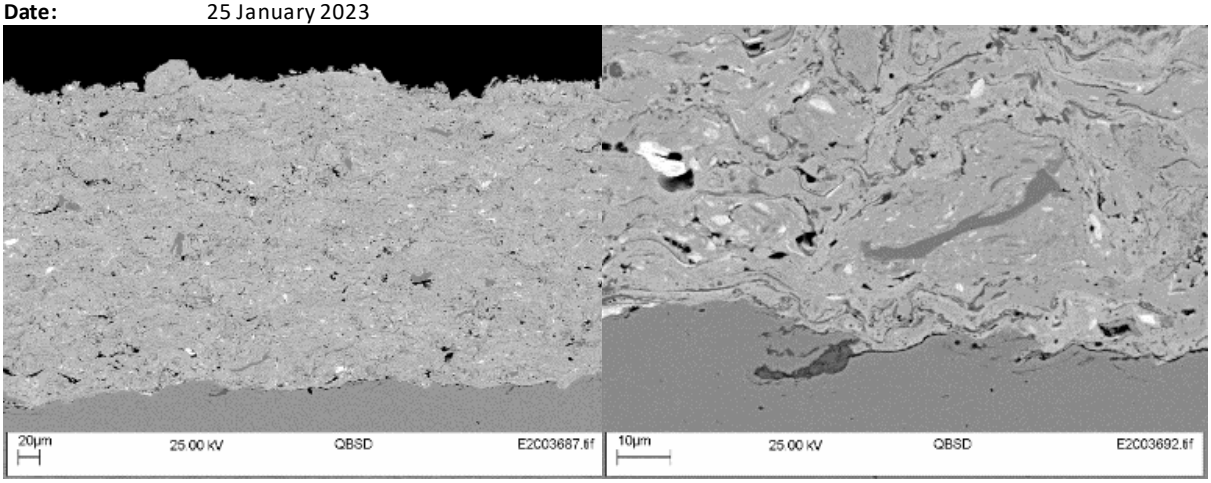

Figure 16 SEM micrographs of Coating 283HEA2 in back-scattered mode

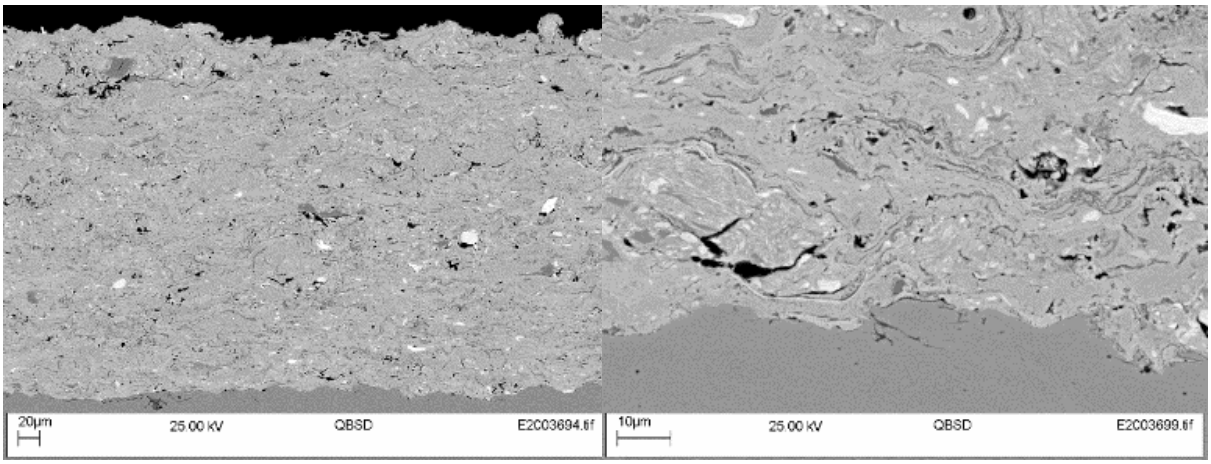

Figure 17 SEM micrographs of Coating 283HEA3 in back-scattered mode

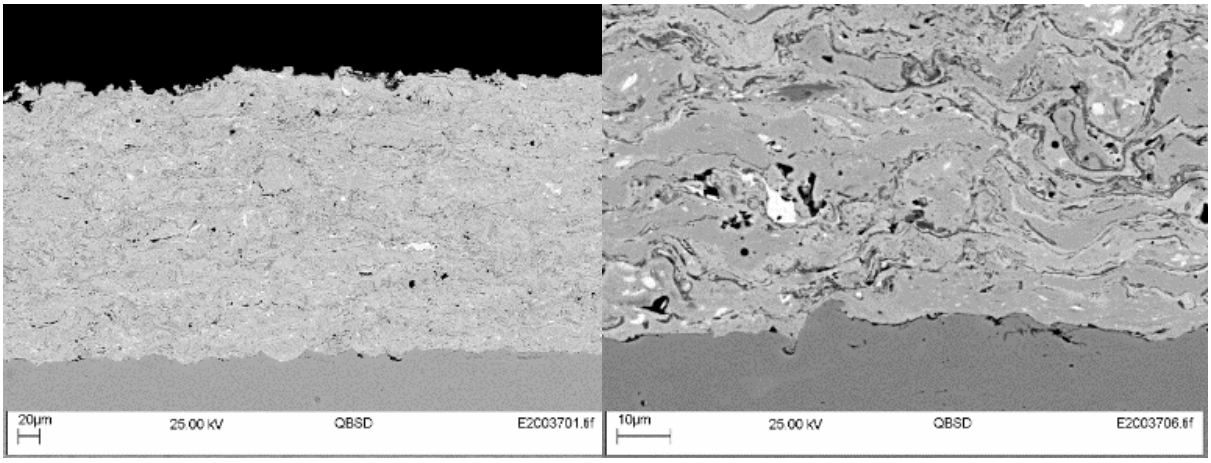

Figure 18 SEM micrographs of Coating 283HEA4 in back-scattered mode

Table 12 As-deposited coating surface roughness of DoE matrix with HEA powder

Run #	Oxygen flow, SLPM	Kerosene flow, SLPM	Ra, µm		Rz, µm	
			Ave	Dev	Ave	Dev
283HEA1	920	0.355	6.4	0.3	43.7	2.1
283HEA2	873	0.330	6.8	0.3	52.9	6.5
283HEA3	873	0.355	6.6	0.3	46.0	5.5
283HEA4	873	0.375	6.3	0.4	48.4	5.1

Table 13 Results of ASTM C633 adhesion test for HEA coatings

Run #	Oxygen flow, SLPM	Kerosene flow, SLPM	Adhesion, MPa	
			Ave	Dev
283HEA1	920	0.355	50.1	10.0
283HEA2	873	0.330	43.7	8.0
283HEA3	873	0.355	59.2	16.2
283HEA4	873	0.375	50.3	10.5

Table 14 Test results of DoE matrix with HEA powder

Run #	Oxygen flow, SLPM	Kerosene flow, SLPM	Porosity, %		D.E., %	Hardness, $HV_{0.3}$	
			Ave	Dev	%	Ave	Dev
283HEA1	920	0.355	1.6	0.3	52	575	48
283HEA2	873	0.330	1.8	0.5	59	569	60
283HEA3	873	0.355	1.6	0.3	61	558	61
283HEA4	873	0.375	1.2	0.3	57	528	58

4. PRODUCTION OF TEST SAMPLES

A number of test coupons have been produced for the first round of testing in WP3. The first round of test coupons produced for WC-CrC-Ni and HEA coatings includes 12 adhesion test coupons (both 34CrNiMo6 (EN24T) and 440B substrates, 6 off each), 5 slurry test coupons (34CrNiMo6 (EN24T) substrate), 5 wear-rotation test coupons (34CrNiMo6 (EN24T) substrate), 10 corrosion test coupons (34CrNiMo6 (EN24T) substrate), and 8 erosion-corrosion test coupons (34CrNiMo6 (EN24T) substrates). WC-Ni coating was only produced for erosion-corrosion testing on hammer bit steel, 835M30, as addressed in PR1 report. The coupons were prepared using the following:

- Equipment: JP5000 HVOF system (as described in Section 2.2);
- Substrates prepared as described in Section 2.1.2.

Table 15 summarises the process conditions and expected coating properties. More test coupons will be prepared for further testing such as ring-on-ring, tribo-corrosion etc once results from the first round are released and discussed.

Table 15 Process parameters and expected properties for test coupons for first round of WP3 testing *

	WC-Ni coatings	WC-CrC-Ni coatings	HEA coatings
ID	281WC	282WCr	283HEA
Powder	SX477	SX199	HEA (CoCrFeNiMo0.85)
Powder TWI ID	4286	4287	4293
Run conditions	281WC3	282WCr4	283HEA3
Spray angle, °	90	90	90
Powder carrier gas	Argon	Argon	Argon
Gun traverse speed, mm/s	900	900	900
Increment, mm	5	5	5
Number of passes	45	30	36
Specimen cooling	Air	Air	Air
Nozzle	6 inch	6 inch	4 inch
Powder feeder	Three-way	Three-way	Three-way
Powder feed rate, rpm	350	250	150
Carrier gas flow rate, scfh	28	28	28
Spray distance, mm	350	350	355
Oxygen flow, SLPM	920	920	873
Kerosene flow, SLPM	0.375	0.350	0.355
Surface roughness (Ra), µm	3.9±0.2	6.1±0.2	6.6±0.3
Porosity, %	2.0±0.4	1.8±0.2	1.6±0.3
Hardness, $HV_{0.3}$	1077±60	994±121	558±61
Adhesion strength, MPa	-	-	59.2±16.2

Note: * coating characteristics are subject to being deposited on bright mild steel; they may vary if a different substrate material is being used.

5. CONCLUSIONS

Both cermet and high entropy alloy (HEA) coatings were synthesised in this task through HVOF spraying, and a preferred process was selected based on their microstructure and hardness. The following three coatings with the best overall characteristics such as high density, good hardness, etc, were selected for testing in WP3:

- WC-Ni coating, with average surface roughness of 3.9±0.2µm, porosity of 2.0±0.4%, and hardness of 1077±60$HV_{0.3}$.
- WC-CrC-Ni coating, with average surface roughness of 6.1±0.2µm, porosity of 1.8±0.2%, and hardness of 994±121$HV_{0.3}$.
- HEA coating, with average surface roughness of 6.6±0.3µm, porosity of 1.6±0.3%, and hardness of 558±61$HV_{0.3}$.

These coatings have been used to produce test coupons for the first round of testing in WP3. More test coupons will be prepared for further testing such as ring-on-ring, tribo-corrosion etc once results from the first round are released and discussed.

REFERENCES

[1] N A Ahmad, Z Kamdi, Z. Mohamad, A S Omar, N Abdul Latif, A L Mohd Tobi. Characterization of WC-10Ni HVOF Coating for Carbon Steel Blade. IOP Conference Series: Materials Science and Engineering 2017, 165.

[2] Q Wang, Y Zhang, X Ding, S Wang, C.S Ramachandran. Effect of WC Grain Size and Abrasive Type on the Wear Performance of HVOF-Sprayed WC-20Cr3C2-7Ni Coatings.Coatings, 2020, 10: 660.

[3] A SM Ang, C C Berndt, M L Sesso, A Anupam, S Praveen, R S Kottada, B S Murty. Plasma-Sprayed High Entropy Alloys: Microstructure and Properties of AlCoCrFeNi and MnCoCrFeNi. Metall Mater Trans A. 2015, 46:791–800.

[4] S Chen, Y Tong, P K Liaw. Additive Manufacturing of High-Entropy Alloys: A Review.Entropy 2018,20: 937.

[5] X H Yan, J S Li, W R Zhang, Y Zhang. A brief review of high-entropy films. Materials Chemistry and Physics, 2018, 210: 12.